



HAL
open science

Interaction between glyphosate and dissolved phosphorus on bacterial and eukaryotic communities from river biofilms

Louis Carles, Joan Artigas

► **To cite this version:**

Louis Carles, Joan Artigas. Interaction between glyphosate and dissolved phosphorus on bacterial and eukaryotic communities from river biofilms. *Science of the Total Environment*, 2020, 719, pp.137463. 10.1016/j.scitotenv.2020.137463 . hal-02998700

HAL Id: hal-02998700

<https://hal.science/hal-02998700>

Submitted on 20 Nov 2020

HAL is a multi-disciplinary open access archive for the deposit and dissemination of scientific research documents, whether they are published or not. The documents may come from teaching and research institutions in France or abroad, or from public or private research centers.

L'archive ouverte pluridisciplinaire **HAL**, est destinée au dépôt et à la diffusion de documents scientifiques de niveau recherche, publiés ou non, émanant des établissements d'enseignement et de recherche français ou étrangers, des laboratoires publics ou privés.

26 **Abstract**

27 Since the capacity of river biofilms to degrade glyphosate has been proven to increase when
28 the availability of dissolved phosphorus (P) in water decreases, the present study investigates
29 the diversity responses of bacterial and eukaryotic microbial communities from biofilms in a
30 search for glyphosate-degrader candidates. Glyphosate and P interactions were observed for
31 eukaryotic communities, the highest community richness and diversity being preserved at low
32 concentrations of glyphosate and P. This trend marked by glyphosate was also observed in the
33 structure of eukaryotic communities. Therefore, phosphorus and glyphosate had a synergistic
34 effect in decreasing the richness and diversity of eukaryotes species in biofilms. However,
35 species richness and diversity in bacterial communities were not affected by glyphosate,
36 though shifts in the structure of these communities were concomitant with the degradation of
37 the herbicide. Bacterial communities capable of using glyphosate as P source were
38 characterized by increases in the relative abundance of certain Bacteroidetes, Chloroflexi,
39 Cyanobacteria, Planctomycetes and alpha-Proteobacteria members. Glyphosate-degrader
40 candidates found in natural river biofilms can be further isolated for better understanding of
41 glyphosate degradation pathways, and used as bioremediation strategies in heavily
42 contaminated sites.

43

44 **Keywords**

45 AMPA; alpha-Proteobacteria; Cyanobacteria; mineralization; soluble reactive phosphorus;
46 microcosm.

47

48

49

50

51

52 **1 Introduction**

53 Since the middle of the twentieth century, anthropic activities continuously introduce a huge
54 diversity of xenobiotic compounds into the environment. The Intergovernmental Science-
55 Policy Platform on Biodiversity and Ecosystem Services (IPBES, 2018) report a continuous
56 strong decline in biodiversity in Europe and Central Asia, partly explained by intensive
57 agriculture and forestry practices used to increase the provision of food and biomass-based
58 fuels. The interaction between anthropic activities and climate change places rivers as among
59 the most threatened ecosystems in the biosphere both in terms of species extinction and losses
60 in ecosystem services. While the vulnerability of animal and plant biodiversity to global
61 change has been demonstrated in freshwater ecosystems (*e. g.* Strayer and Dudgeon (2010)),
62 the response of microbial biodiversity to these impacts is often neglected.

63 Glyphosate (N-(phosphonomethyl) glycine) is a systemic herbicide inhibiting aromatic
64 amino acid biosynthesis in plants. Since first introduced in the early 70's, and as a result of its
65 high weed prevention efficiency, glyphosate use has increased rapidly (Duke, 2015). This
66 herbicide has become the most frequently used active substance in most countries worldwide
67 (Benbrook, 2016), as well as in France (AGRESTE, 2018). Consequently, glyphosate and its
68 main primary metabolite AMPA (aminomethyl phosphonic acid) have become among the
69 compounds most frequently quantified in river waters (43% and 63% quantification frequency
70 in France from 2012 to 2016, respectively) (NAIADES, 2018). Glyphosate use is authorised
71 in Europe (included in Annex I to Directive 91/414/EEC on 2002/07/01 by Commission
72 Directive 2001/99/EC) and 192 glyphosate-based formulations are currently approved in
73 France (E-Phy, 2018). However, the broad contamination of the environment by glyphosate
74 has recently prompted the authorities to question the extension of its authorisation, by taking

75 into account its potential harmful side effect to human and ecosystems health (Davoren and
76 Schiestl, 2018; Van Bruggen et al., 2018).

77 Once in rivers, glyphosate can interact with microbial biofilms which have a certain
78 sensitivity to this herbicide. Biofilms are natural consortia of microorganisms composed of
79 bacteria, algae, fungi and protozoa embedded in an extracellular matrix protecting them
80 against environmental stressors such as nutrient starvation and pollutants (Besemer, 2015).
81 Bonnineau et al. (2012) showed a stronger decrease in photosynthetic efficiency in shade-
82 adapted biofilms (half maximal effective concentration $EC_{50} = 11.7 \text{ mg L}^{-1}$) than in high-
83 light adapted biofilms ($EC_{50} = 35.6 \text{ mg L}^{-1}$) exposed to glyphosate. Accordingly, light history
84 can influence the structure and composition of phototrophic populations in biofilms, and thus
85 modulate their photosynthetic response to the herbicide. Other studies also revealed a negative
86 impact of glyphosate in terms of phototrophic community growth when exposed to $10 \text{ } \mu\text{g L}^{-1}$
87 of glyphosate (Bricheux et al., 2013) and significant decreases in biomass, primary production
88 and heterotroph community respiration when exposed to 2.5 g L^{-1} of glyphosate (Shaw and
89 Mibbayad, 2016). Within phototrophic communities, diatoms appear as the most sensitive
90 group to the herbicide, while cyanobacteria and chlorophyte are the least sensitive (Vera et al.,
91 2010). However, exposure of river biofilms to low concentrations of glyphosate ($<100 \text{ } \mu\text{g L}^{-1}$)
92 did not significantly affect algal and bacterial growth (Carles et al., 2019) and even slightly
93 increased their biomass production (Klátyik et al., 2017). A recent study has provided
94 evidence of the involvement of glyphosate in phosphorus (P) recycling by riverine biofilms
95 (Carles et al., 2019). Phosphorus-starved biofilms are capable of mineralising glyphosate and
96 therefore use the P contained in the herbicide molecule ($\text{C}_3\text{H}_8\text{NO}_5\text{P}$) for metabolism.
97 However, P enriched biofilms tended to transform glyphosate into AMPA ($\text{CH}_6\text{NO}_3\text{P}$) the
98 latter accumulating in the media, as well as in biofilm (Fernandes et al., 2019), thus
99 contributing to P eutrophication of river waters.

100 Herbicide tolerance can use either low cell permeability or the occurrence of detoxifying
101 enzymes or degradative pathways. Research addressing glyphosate tolerance has been mostly
102 focused on microbial populations rather than on multi-species biofilms. At the population
103 level, contrasted responses to glyphosate were obtained depending on the isolated strain. The
104 herbicide tends to favour the biofilm formation of *Pseudomonas aeruginosa* (Lima et al.,
105 2014) while no significant effect was observed on the biofilm formation of *Clavibacter*
106 *michiganensis* ssp. *sepedonicus* (Perfileva et al., 2018). Glyphosate tolerance has been
107 explained in *Escherichia coli* by the overexpression of a membrane transporter involved in
108 drug efflux, which reduces intracellular accumulation of the herbicide (Staub et al., 2012).
109 Bacteria could also overcome some of the harmful effects of glyphosate by increasing the
110 production of molecules that scavenge free radicals (Liu et al., 2013). A strong tolerance of
111 several cyanobacterial strains has also been pointed out in cyanobacterial strains possessing
112 an insensitive form of the glyphosate target EPSPS (5-enol-pyruvyl-shikimate-3-phosphate
113 synthase (Forlani et al., 2008)). Finally, the biodegradation of glyphosate by bacterial strains
114 also highlights the capacity of microorganisms to use this herbicide for their growth. The
115 relationships between glyphosate biodegradation is well described for soil and sludge
116 microorganisms (Sviridov et al., 2015). Among various glyphosate-degrading
117 microorganisms, bacteria play the most pivotal role, and the processes of glyphosate
118 biodegradation have therefore been well studied (Zhan et al., 2018). Most of the glyphosate-
119 degrading strains described so far use the herbicide as a source of phosphorus, which implies
120 that they possess enzymes cleaving the C–P bond. Two main pathways for enzymatic
121 biodegradation of glyphosate have therefore been found in bacteria: direct cleavage of the C–
122 P bond, yielding sarcosine and inorganic phosphorus (sarcosine pathway), and cleavage of the
123 C–N bond, yielding glyoxylate and AMPA (AMPA pathway) (Sviridov et al., 2015).
124 Microorganisms that use glyphosate as a phosphorus source via the sarcosine pathway possess

125 the enzymatic CP-lyase complex (Hove-Jensen et al., 2014). The genes encoding the
126 corresponding enzymes are assembled into the *phn* operon, which is widespread among
127 bacterial species such as *Achromobacter* sp. MPS 12A (Sviridov et al., 2012) and
128 *Arthrobacter* sp. GLP-1 (Pipke et al., 1987). In the other main glyphosate biodegradation
129 pathway (AMPA pathway), the herbicide molecule is first attacked by the enzyme glyphosate
130 oxidoreductase (GOR), which cleaves the C–N bond in the glyphosate molecule, leading to
131 stoichiometric quantities of AMPA and glyoxylate (Sviridov et al., 2015). In most glyphosate-
132 degrading bacteria, glyoxylate enters the glyoxylate bypass of the Krebs cycle, while AMPA
133 is exported into the extracellular space. This pathway has been extensively studied in
134 *Ochrobactrum anthropi* GPK 3 (Sviridov et al., 2012), and was also described in several other
135 bacteria such as *Pseudomonas* sp. SG-1 (Talbot et al., 1984) and *Agrobacterium radiobacter*
136 SW9 (Mcauliffe et al., 1990).

137 Specific microbial populations involved in glyphosate degradation in natural river
138 biofilms are largely unknown. Therefore, the present study sought to determine the interaction
139 effect of glyphosate and dissolved phosphorus on the structure and composition of bacterial
140 and eukaryotic communities in biofilms and identify taxa potentially involved in glyphosate
141 degradation. Mi-seq Illumina sequencing analyses have been performed on biofilm samples
142 collected from the previous study by Carles et al. (2019). This work studied contrasted
143 biofilms from an upstream site (not exposed to glyphosate) and a downstream site
144 (chronically exposed to glyphosate) exposed to different phosphorus (low_P versus high_P)
145 and glyphosate (low_G versus high_G) concentrations in water. Taxonomic groups in
146 biofilms linked to glyphosate biodegradation have been described and compared to the known
147 glyphosate-degrading microorganisms present in the literature. Our main hypotheses were: i)
148 the structure and composition of microbial communities in biofilms, and especially that of
149 algal populations, will be modified with increased glyphosate concentrations in water; and ii)

150 low dissolved phosphorus availability would favour the development of glyphosate-degrading
151 taxa in biofilms, while high dissolved phosphorus availability would eventually favour the
152 proliferation of taxa capable of transforming the glyphosate into AMPA.

153

154 **2 Materials and Methods**

155

156 *2.1 Experimental design*

157 A microcosm study was conducted in the laboratory with natural biofilms grown in the field
158 at the end of spring 2017, as described by Carles et al. (2019). Briefly, biofilms grown on
159 glass slides at an upstream site (Ups) and a downstream site (Dws) of the Artière River (Puy-
160 de-Dôme region, France) were placed in 24 microcosms consisting of 20 L glass aquariums.
161 Half of the aquaria received Ups biofilms, while the other half received Dws biofilms. After
162 two weeks of biofilms' acclimation to microcosms in their corresponding river water, each
163 type of biofilm (Ups and Dws) was subjected to the four experimental conditions in triplicate
164 depending on the water phosphorus concentration (LowP = 100 $\mu\text{g P L}^{-1}$ and HighP = 1000
165 $\mu\text{g P L}^{-1}$ and glyphosate concentration (LowG = 10 $\mu\text{g L}^{-1}$ and HighG = 100 $\mu\text{g L}^{-1}$). Briefly,
166 water from the upstream site of the Artière (low dissolved phosphorus concentration and
167 absence of glyphosate; (Rossi et al., 2019)) was used to fill all microcosms which were later
168 contaminated by phosphorus (K_2HPO_4 , ACS reagent) and glyphosate (PESTANAL[®],
169 analytical standard) depending on the experimental conditions described above. These
170 experimental conditions correspond to 1x and 10x the mean of actual concentration of
171 glyphosate in surface waters from France. The experimental conditions in our microcosm
172 experiment were therefore chosen to assess realistic environmental contamination conditions.
173 Neither photolysis nor adsorption of glyphosate in the microcosms were observed during the
174 experiment (Carles et al., 2019). Water and biofilm analyses were carried out at days 0, 2, 4,

175 6, 13, and 27 post-contamination. One glass slide (28 × 83 mm) was removed from each
176 aquarium at each sampling time and scraped in sterile conditions. Scraped biofilms were
177 conserved frozen (- 20 °C) until DNA analysis. Dissolved nitrate and phosphorus
178 concentrations in water from aquariums were maintained throughout the experiment by
179 adding adequate salt solution volumes of 1 M KNO₃ and 1 M K₂HPO₄ respectively. Further
180 details of physico-chemical and microbial parameters measured in this experiment can be
181 found in Carles et al. (2019).

182

183 2.2 *Nucleic acids extraction and sequencing*

184 Nucleic acid extraction was carried out on selected dates (depending on glyphosate
185 biodegradation results from Carles et al. (2019)): days 0, 6, 13 and 27. Total DNA extraction
186 was performed from 1 mL of scraped biofilm suspension using the FastDNATM Spin Kit for
187 soil (MP Biomedicals, Santa Ana, CA, USA) following the manufacturer's recommendation.
188 Quantification and quality checking of extracted DNA was carried out using a Nanodrop
189 (260/230 and 260/280 ratios; NanodropTM 2000, Wilmington, DE, U.S.A.) and
190 electrophoresis on 1% agarose gel.

191 Further sample processing and sequencing was performed by the University of Illinois
192 Keck Center (Urbana, USA). Briefly, sequencing (MiSeq bulk 2 x 250 bp, 10M-20M paired
193 reads on Illumina MiSeq platform) yielded a total of 4,117,394 reads (Eukaryotes) and
194 13,244,386 reads (Prokaryotes). Specific primers used for PCR were Euk_1391f (5'-
195 GTACACACCGCCCGTC) / EukBr (5'-TGATCCTTCTGCAGGTTACCTAC) for
196 Eukaryotes (Gilbert et al., 2014) and V4_515F_New (5'-GTGYCAGCMGCCGCGGTAA) /
197 V4_806R_New (5'-GGACTACNVGGGTWTCTAAT) for Prokaryotes (Caporaso et al.,
198 2011). Sample inference from amplicon data was carried out using DADA2 pipeline (Version
199 1.8, <https://bioconductor.org/biocLite.R>). The DADA2 pipeline (Callahan et al., 2016)

200 consists of amplicon sequence variants (ASVs) inference, replacing the coarser and less
201 accurate OTU clustering approach (Callahan et al., 2017). ASV methods have demonstrated
202 sensitivity and specificity as good as or better than OTU methods and better discriminate
203 ecological patterns (Amir et al., 2017; Callahan et al., 2016; Edgar, 2016; Eren et al., 2015,
204 2013; Tikhonov et al., 2015). Sequence variants and their sample-wise abundances were
205 generated from the demultiplexed fastq files after removing substitution and chimera errors.
206 Taxonomic classification was carried out via a native implementation of the RDP naive
207 Bayesian classifier, and species-level assignment to 16S rRNA gene fragments by exact
208 matching. The corresponding sequence files were deposited in NCBI's Sequence Read
209 Archive (SRA BioProject ID, PRJNA596462).

210

211 *2.3 Data analyses*

212 Data analyses were performed using RStudio (Version 1.1.456) implemented with the
213 Phyloseq package (version 1.24.0). After rarefaction, bacterial and eukaryotic datasets were
214 composed of samples containing the same number of reads (41085 and 11315 reads,
215 respectively). Rarefaction curves were plotted using the ggplot2 package (version 3.0.0) from
216 community analyses made with the vegan package (version 2.5-2). Shannon index and Chao1
217 species richness were determined with Phyloseq package. PERMANOVA tests were carried
218 out on the weighted unfrac distances matrix of bacterial and eukaryotic communities using
219 the R package "vegan". After testing homogeneity in bacterial and eukaryotic datasets
220 dispersion, the adonis function was used to test the null hypothesis to see if experimental
221 treatments shared similar centroids.

222 The correlation between each ASV abundance and the glyphosate or AMPA concentration
223 at each sampling time (days 0, 6, 13, and 27) has been established for bacteria and Eukaryotes
224 using the Spearman's rank correlation test. Then, the 10 highest negatively correlated ASVs

225 with glyphosate concentration ($r < -0.69$) were included in 16S and 18S phylogenetic
226 analyses, in comparison to the sequences of known isolated glyphosate-degrading strains (or
227 closest sequences retrieved from the GenBank database). The phylogenetic analysis was
228 carried out by multiple alignments (Clustal Ω) followed by the construction of phylogenetic
229 trees using MEGA X software (Kumar et al., 2018).

230 Analyses of variance were carried out using RStudio (Version 1.1.456). The fixed factors
231 (modalities) were as follow: Site (Ups, Low P-content and Dws, High P-content); Glyphosate
232 in water (LowG and HighG concentration); dissolved P availability in water (LowP and
233 HighP water); Time (6, 13 and 27 days). The influence of these factors was tested on various
234 dependent variables linked to diversity indexes (Chao1 and H') and shifts in microbial
235 community structure (mean rate of change) were assessed using three/four-way ANOVA
236 followed by separate post hoc comparisons (Tukey's test, $P < 0.05$). The four-way ANOVA
237 includes the factors described above and Time (6, 13 and 27 days). The normality and
238 homogeneity of variance were checked prior to ANOVA tests (Shapiro's and Levene's tests,
239 respectively, $P < 0.05$) and data not normally distributed were transformed using logarithmic,
240 square, square root or Box-Cox functions.

241

242 **3 Results and Discussion**

243

244 *3.1 Glyphosate and/or Phosphorus effect on communities structure*

245 3.1.1 Initial community structure and composition of biofilms

246 The total number of ASVs identified by 16S and 18S rRNA genes sequencing was 41085
247 and 11315, for Bacteria and Eukaryotes respectively. Each microbial community was well
248 covered by the sequencing, as attested by the inflections in the rarefaction plots of the
249 different biofilm samples (Figure S1).

250 At the beginning of the experiment, a total of 29 and 22 bacterial phyla were detected in
251 upstream and downstream biofilms respectively (Figure 1A and S2A). Unclassified sequences
252 represented less than 0.3% of the total number of ASVs in both biofilm types. Globally, the
253 bacterial communities were dominated by 3 phyla, representing 83.8% of the total number of
254 ASVs, including Proteobacteria (59.4%), Cyanobacteria (16.3%) and Bacteroidetes (8.1%)
255 (Figure 1A). These three phyla are generally dominant in stream biofilms (Battin et al., 2016),
256 Proteobacteria often being the most common (Liao et al., 2019; Peng et al., 2018).

257 However, some differences were observed depending on the site on which the biofilm was
258 grown. Indeed, the environmental template between upstream and downstream sites was
259 consistently different; the downstream site presented higher concentrations than the upstream
260 site in terms of dissolved inorganic phosphorus (0.32 and 0.03 mg P L⁻¹, respectively),
261 organic carbon (12.97 and 6.50 mg DOC L⁻¹ respectively), glyphosate (0.25 and 0 µg L⁻¹
262 respectively) and AMPA (1.08 and 0.09 µg L⁻¹ respectively) (see Rossi et al. 2019). A total of
263 21 phyla were common to both sites, with 8 phyla specific to upstream and 1 phyla specific to
264 downstream. Moreover, Cyanobacteria were more frequent in downstream (25.9%) than
265 upstream biofilms, likely due to the higher phosphorus concentration in the downstream site
266 compared to the upstream one. Cyanobacteria are also able to tolerate glyphosate, which has
267 higher concentrations downstream than upstream. This tolerance has been explained by the
268 presence of a resistant form of EPSPS in cyanobacteria and the ability of some strains to
269 metabolize glyphosate (Arunakumara et al., 2013; Drzyzga and Lipok, 2018; Forlani et al.,
270 2008). Inversely, Bacteroidetes was less common in downstream (4.2%) than upstream (12%)
271 biofilms. It has already been demonstrated that members of the Phyla Bacteroidetes are
272 sensitive to glyphosate, as in the case of human (Dechartres et al., 2019) and honey bees
273 (Motta et al., 2018) gut microbiota.

274 For the eukaryotic communities at day 0, a total of 21 and 18 phyla were detected in
275 upstream and downstream biofilms respectively (Figure 1B and S2B). Unclassified sequences
276 accounted for 40.7% (upstream) and 24.4% (downstream) of the total number of ASVs.
277 Globally, eukaryotic communities were dominated by 4 phyla, accounting for 58.1% of the
278 total number of ASVs (Figure 1B). These phyla were Ochrophyta (23.5%), Chlorophyta
279 (13.7%), Ciliophora (10.5%) and Annelida (10.4%). A total of 14 phyla common to both
280 biofilm types were detected, while 6 phyla were only detected in the upstream biofilm and 4
281 in the downstream one. For example, Ciliophora was one of the dominant phyla in the
282 upstream biofilm (20.3%), whereas it was almost absent from the downstream one (0.6%).
283 Different sensitivity levels of Ciliates with respect to glyphosate have been reported in the
284 literature (Bonnet et al., 2007; Everett and Dickerson, 2003; Tsui and Chu, 2003), indicating
285 that, in the present study, the presence of glyphosate by itself cannot explain the variation of
286 Ciliophora abundance between upstream and downstream biofilms.

287 Conversely, Annelida and Chlorophyta were well represented in the downstream site
288 (20.8% and 26.5%, respectively), while they absent or only accounted for 0.8% in the
289 upstream site respectively. Both phyla are known to tolerate eutrophic conditions quite well,
290 which is consistent with the higher nutrient and organic carbon concentrations found in the
291 downstream site compared to the upstream site (Rossi et al. 2019). Moreover, these phyla
292 seem to be insensitive to glyphosate. The few studies available in the literature exposed
293 organisms to unrealistic (excessively high) glyphosate concentrations. For example, a study
294 showed some adverse effects on two species of Annelids at concentrations that greatly exceed
295 the recommended field application rate of glyphosate (García-Torres et al., 2014). Besides,
296 high concentrations of glyphosate (order of mg L^{-1}) decreased the abundance of Chlorophytes
297 in the periphyton (Gonzalez et al., 2019).

298 Differences between downstream and upstream eukaryotic communities can be explained
299 by xenobiotics pressure, as well as other chemical stressors, such as increased availability of
300 dissolved carbon and nutrients (Van Horn et al., 2011) which support the “paradox of
301 enrichment” phenomenon in aquatic microbial communities (*e. g.* Tubay et al. (2013)).

302

303 3.1.2 Responses of richness and diversity in microbial communities

304 At the beginning of the experiment, Ups biofilms showed higher bacterial and eukaryotic
305 species richness (Tukey, $P < 0.05$) and diversity (Tukey, $P < 0.05$) compared to the Dws ones,
306 and this site effect was maintained for Eukaryotes after 6 days of incubation (Table 1 and
307 Figure S3, $P < 0.05$). Moreover, a decrease in eukaryotic species richness ($P < 0.05$) and
308 diversity ($P < 0.05$) was observed over time, as well as for bacteria, in Dws communities
309 (time \times site interaction, $P < 0.01$). Low species richness and diversity in downstream
310 communities can be explained by xenobiotics and nutrients pressure (Van Horn et al., 2011).
311 However, downstream communities that are expected to be more acclimated to glyphosate are
312 those that experience the greatest decrease in eukaryotes richness and diversity after exposure
313 to glyphosate (Table 1).

314 Dissolved phosphorus treatments were not essentially affecting microbial diversity indices
315 in biofilms (Table 1 and Figure S3C, $P > 0.05$), with the exception of eukaryotic
316 communities, that slightly decreased their species richness under HighP water on certain
317 sampling dates (days 6 and 13) compared to day 0 (Time \times P_{water} interaction, $P < 0.01$).
318 However, the structure of both bacteria and Eukaryotic communities responded to dissolved
319 phosphorus treatments at the beginning of the experiment (day 6) compared to later sampling
320 dates (Figure S4; PERMANOVA, Time \times P_{water} interaction, $P < 0.05$ and 0.01,
321 respectively).

322 A higher eukaryotic species richness ($P < 0.001$) and diversity ($P < 0.001$) has been
323 observed after 6, 13 and 27 days for LowG compared to HighG conditions (Table 1 and
324 Figure S3, $P < 0.05$). This trend marked by the glyphosate was also observed in the structure
325 of eukaryotic communities (Figure S4, PERMANOVA Gwater effect, $P < 0.01$, Table S1).
326 Interactions between Pwater and Gwater were observed for Eukaryotic species richness ($P <$
327 0.05), diversity ($P < 0.01$) but not for the structure of this community (PERMANOVA Pwater
328 x Gwater interaction, $P = 0.059$, Table S1). The highest diversity was observed in lowP_lowG
329 treatments for both upstream and downstream communities. According to our results, the
330 interaction (lowP_lowG) was significant for eukaryotic communities. We could conclude that
331 P and glyphosate had a synergistic effect in decreasing eukaryotes species richness and
332 diversity in biofilms. No conclusions can be drawn for prokaryotes.

333 Neither the species richness nor the diversity of bacterial communities were affected by
334 the two glyphosate concentrations tested ($P = 0.812$ and $P = 0.712$, respectively).
335 PERMANOVA tests revealed also that glyphosate did not significantly modify bacterial
336 communities structure (Gwater effect, $P = 0.054$; Figure S4 and Table S1). The decrease of
337 richness and diversity in the presence of high concentration of glyphosate was only observed
338 for Eukaryotic communities, which are potentially targeted by the herbicide. Indeed, The
339 physiological and biochemical similarities between algae and terrestrial plants suggest that
340 algae would be particularly vulnerable to glyphosate (Annett et al., 2014). Moreover, this
341 impact in HighG water could explain the higher impact in HighP water, in which glyphosate
342 effects are more consistent on days 13 and 27 in Eukaryotic communities.

343 On the basis of these results, it could be supposed that the most promising area to find
344 glyphosate-degrading strains could be within the bacterial community. Bacterial richness and
345 diversity were weakly modified, so more tolerant to glyphosate, than the Eukaryotic ones. The
346 most promising communities are certainly those exposed to LowP and LowG water. There are

347 two main reasons according to Carles et al. (2019): (i) glyphosate degradation is accelerated
348 when dissolved phosphorus availability in water is low, and (ii) glyphosate is completely
349 removed, without accumulation of AMPA, in this condition.

350 3.1.3 Shifts in microbial communities structure

351 Unifrac coordinates were used to calculate the mean rate of change in the structure of the
352 microbial community in experimental conditions over the duration of the experiment (Figure
353 S5). Overall, the rate of change in bacterial communities was much slower than that observed
354 for the eukaryotic ones. Eukaryotic community structure of biofilms in LowP water changed
355 faster than the HighP one ($P < 0.01$). Moreover, the microbial community structure was
356 modified more quickly for biofilms exposed to LowG compared to HighG (Figure S4, $P <$
357 0.05 (Bacteria), $P < 0.01$ (Eukaryotes)). The interaction between dissolved phosphorus and
358 glyphosate ($P < 0.05$ (Bacteria), $P < 0.001$ (Eukaryotes)) revealed that both type of biofilms
359 (Ups and Dws) undergo the highest rate of change when exposed to LowP and LowG (Figure
360 S5).

361 The lower concentration of glyphosate in water induces the fastest shifts in the microbial
362 community structure. The plasticity of the microbial community structure seems to be higher
363 in the case of low doses of pollutant. Despite the relatively high EC_{50} of glyphosate (11.7 –
364 35.6 mg L⁻¹ found by Bonnineau et al. (2012) with regard to the photosynthetic efficiency of
365 biofilm, a negative impact of glyphosate on phototrophic community growth has been
366 observed for biofilms exposed to 10 µg L⁻¹ of glyphosate (Bricheux et al., 2013). The results
367 of our study probably reflect an exposure to a sub-lethal dose enabling for better tolerance to
368 glyphosate. The response was more marked on eukaryotes, which most likely possess the
369 class I of EPSPS, the sensitive form of EPSPS towards glyphosate (Annett et al., 2014). There
370 is also a strong effect of phosphorus, indicating that a higher trophic state can lower the
371 adaptation of microbial communities or override the effect of glyphosate.

372 In that sense, we confirm our focus on the LowP_LowG condition showing the fastest
373 adaptation capacity in the search for glyphosate degraders. Moreover, it was also shown that
374 the fastest glyphosate dissipation (lowest dissipation times 50%, DT_{50s}) was obtained with
375 biofilms in LowP_LowG microcosms (Carles et al., 2019).

376

377 3.2 *Glyphosate-degrading microorganisms in biofilms*

378 As mentioned above, we further analysed microbial diversity in the most efficient
379 condition for glyphosate degradation without AMPA accumulation (LowP_LowG) taking into
380 account ASVs abundance data from days 6, 13, and 27.

381 3.2.1 Relationships between ASVs and glyphosate and AMPA

382 The correlation between each ASV abundance and glyphosate concentration over time has
383 been plotted against the correlation between this ASV abundance and AMPA concentration
384 (Spearman's rank correlation). Then, an additional correlation test revealed a positive linear
385 relationship between ASVs abundance correlations with glyphosate and AMPA (Figure 2), as
386 attested by the values of the Spearman's rank correlation test (Eukaryotes, $\rho = 0.809$, $P <$
387 0.001 ; bacteria, $\rho = 0.832$, $P < 0.001$). These results highlight a linear distribution of
388 microorganisms from those characterized by high ASVs abundance in the presence of high
389 concentrations of glyphosate and AMPA (positive Spearman's correlation) to the ones that
390 correspond to high ASVs abundance in the presence of low concentrations of glyphosate and
391 AMPA (negative Spearman's correlation). The last were selected to search for potential
392 glyphosate degradation candidates since they were present at high abundances until the
393 complete depletion of glyphosate and AMPA molecules in the microcosms.

394

395 3.2.2 Taxonomic repartition of the correlation between ASVs abundance and glyphosate

396 3.2.2.1 *Eukaryotes*

397 The repartition of the correlations between ASVs abundance depends on the Phylum
398 (Figure S6). Some of the most abundant phyla, such as Chlorophyta and Ochrophyta, present
399 a large variation in terms of the correlation between the abundance of their ASVs and the
400 concentration of glyphosate in the water. Only three Phyla (Chlorophyta, Cryptomycota and
401 Ochrophyta) contain ASVs abundance that are highly negatively correlated with glyphosate ($-$
402 $0.84 < \text{Spearman's rank coefficient} < -0.69$). Seven of the 10 highest negatively correlated
403 ASVs belong to the Chlorophyta phylum. The abundance of Chlorophyta has been seen to
404 increase and those of Bacilliarophyceae (diatoms) to decrease in periphytic biofilms treated
405 with the glyphosate formulation Roundup® (Vera et al., 2010).

406 Eukaryotic microorganisms described so far for their glyphosate-degrading activity mostly
407 belong to the Ascomycota Phylum (Zhan et al., 2018). However, none of the ASVs belonging
408 to the Ascomycota phylum were found in the top ten ASVs negatively correlated with
409 glyphosate (Figure S7). The present study does not suggest a potential role for Ascomycota
410 members in glyphosate degradation since their ASVs abundances were not strongly
411 negatively correlated with glyphosate. One possible explanation is that Ascomycota are
412 weakly represented in the periphyton since they prefer carbon-rich substrates, such as leaf
413 litter or wood, for growth (Voříšková and Baldrian, 2013). Despite the fact that most
414 Ascomycota members able to degrade glyphosate use this herbicide as a phosphorus source,
415 as in the case of the biofilms in this study, AMPA did not accumulate in the media in the
416 LowP LowG condition. The degradation of glyphosate by Ascomycota described in the
417 literature, which seems to be mainly dominated by the production of AMPA (Zhan et al.,
418 2018), should therefore not be predominant within biofilms.

419

420 3.2.2.2 *Bacteria*

421 Similarly to the Eukaryotic community, the repartition of the correlation between bacterial
422 ASVs abundance depends on the Phylum (Figure S8). Five of the most abundant phyla
423 (Bacteroidetes, Chloroflexi, Cyanobacteria, Planctomycetes and Proteobacteria) contain
424 ASVs abundance that are highly negatively correlated with glyphosate (Spearman's rank
425 coefficient < -0.71).

426 All glyphosate-degrading microorganisms isolated so far come from various environments
427 such as rhizosphere, activated-sludge and glyphosate contaminated soils (Sviridov et al.,
428 2015), while none has been isolated from river biofilms. Interestingly, the present study
429 reveals some ASVs potentially linked to glyphosate biodegradation by river biofilms. Some of
430 them are close to strains able to degrade glyphosate, in terms of 16S phylogeny (Figure 3).

431 For example, one Bacteroidetes member isolated from activated sludge (a *Flavobacterium*
432 strain) is able to use glyphosate as a sole phosphorus source (Balthazor and Hallas, 1986).
433 Alpha-proteobacteria also contains several glyphosate-degrading strains, including the well-
434 studied strain *Ochrobactrum anthropi* GDOS (Hadi et al., 2013). This strain has been isolated
435 from a glyphosate-contaminated soil and is able to use glyphosate as a phosphorus source.
436 Among alpha-proteobacteria, all glyphosate-degrading strains are able to use the herbicide as
437 a sole phosphorus source. Microorganisms that use glyphosate as a phosphorus source possess
438 the enzymatic CP-lyase complex (Hove-Jensen et al., 2014). This enzymatic complex enables
439 an orthophosphate molecule to be released from the glyphosate (sarcosine degradation
440 pathway) or from AMPA (AMPA degradation pathway) (Sviridov et al., 2015). The genes
441 encoding the corresponding enzymes are assembled into the *phn* operon, which is described in
442 *Ochrobactrum anthropi* ATCC 49188 (Hove-Jensen et al., 2014). It is then probable that
443 alpha-proteobacteria candidates for glyphosate degradation in our study (4 ASVs over the ten)
444 use similar enzymatic machinery since AMPA was not an end product in their metabolism.

445 A general tolerance and a remarkable ability to degrade the glyphosate have also been
446 described for cyanobacteria (Forlani et al., 2008; Lipok et al., 2007). Incubations of *Spirulina*
447 *platensis* strain C1 with 10 mM glyphosate concentrations resulted in the disappearance of the
448 herbicide in 14 days concomitantly with the appearance of transient peaks of orthophosphate
449 monoester (Forlani et al., 2008). Chloroflexi are also phototrophic bacteria like cyanobacteria
450 but no studies have shown the presence of strains capable of degrading the glyphosate. On the
451 contrary, a recent publication highlighted that the relative abundance of this phylum tends to
452 decrease in soils treated with glyphosate (Lu et al., 2017).

453 Overall, the ten bacterial ASVs found in LowP and lowG treatment are potential
454 candidates for further glyphosate-bioremediation experiments. However, it has to be noted
455 that our approach can rule out certain ASVs participating in the degradation of glyphosate but
456 present in low ASV abundance when glyphosate is depleted.

457

458 **4 Conclusion**

459 Rivers are continuously affected by various stressors, such as habitat degradation,
460 nutrients and xenobiotics pollution, flow regulation and water abstraction. Studying the
461 stressors, not only separately, but also by taking into account their interactions, gives a more
462 realistic picture of the integrity of ecosystems and their endangered components. In the
463 present study, phosphorus and glyphosate induced differential responses in microbial
464 communities of river biofilms. While eukaryotic communities showed strong diversity
465 plasticity when exposed to low glyphosate concentrations, shifts in the structure of bacterial
466 communities were specifically observed during glyphosate dissipation. Understanding the fate
467 of glyphosate in river ecosystems requires further identification of glyphosate-degrading
468 species from natural microbial communities. Enrichment cultures and isolation of glyphosate-

469 degrading strains will contribute to improving bioremediation actions and the restoration of
470 contaminated areas.

471

472 **5 Acknowledgements**

473 This work was supported by the Agence Nationale de la Recherche (grant number ANR-
474 16-CE32-0001-01 BIGLY). The authors thank Florence Donnadiou and Florent Rossi for
475 their help in water and biofilm sampling and Muriel Joly for her valuable help in diversity
476 analyses.

477

478 **6 Competing interests**

479 The authors declare no competing interests.

480

481 **7 References**

482

- 483 AGRESTE, 2018. Données de vente des produits phytosanitaires 2011 à 2015. [WWW
484 Document]. URL [http://agreste.agriculture.gouv.fr/thematiques-872/productions-](http://agreste.agriculture.gouv.fr/thematiques-872/productions-vegetales-874/grandes-cultures-fourrages-875)
485 [vegetales-874/grandes-cultures-fourrages-875](http://agreste.agriculture.gouv.fr/thematiques-872/productions-vegetales-874/grandes-cultures-fourrages-875) (accessed 5.22.18).
- 486 Amir, A., McDonald, D., Navas-Molina, J.A., Kopylova, E., Morton, J.T., Zech Xu, Z.,
487 Kightley, E.P., Thompson, L.R., Hyde, E.R., Gonzalez, A., Knight, R., 2017. Deblur
488 Rapidly Resolves Single-Nucleotide Community Sequence Patterns. *mSystems* 2.
489 <https://doi.org/10.1128/mSystems.00191-16>
- 490 Annett, R., Habibi, H.R., Hontela, A., 2014. Impact of glyphosate and glyphosate-based
491 herbicides on the freshwater environment. *J. Appl. Toxicol.* 34, 458–479.
492 <https://doi.org/10.1002/jat.2997>
- 493 Arunakumara, K., Walpola, B.C., Yoon, M.-H., 2013. Metabolism and degradation of
494 glyphosate in aquatic cyanobacteria: a review. *Afr. J. Microbiol. Res.* 7, 4084–4090.
- 495 Balthazor, T.M., Hallas, L.E., 1986. Glyphosate-degrading microorganisms from industrial
496 activated sludge. *Appl. Environ. Microbiol.* 51, 432–434.
- 497 Battin, T.J., Besemer, K., Bengtsson, M.M., Romani, A.M., Packmann, A.I., 2016. The
498 ecology and biogeochemistry of stream biofilms. *Nat. Rev. Microbiol.* 14, 251–263.
499 <https://doi.org/10.1038/nrmicro.2016.15>
- 500 Benbrook, C.M., 2016. Trends in glyphosate herbicide use in the United States and globally.
501 *Environ. Sci. Eur.* 28. <https://doi.org/10.1186/s12302-016-0070-0>

502 Besemer, K., 2015. Biodiversity, community structure and function of biofilms in stream
503 ecosystems. *Res. Microbiol.* 166, 774–781.
504 <https://doi.org/10.1016/j.resmic.2015.05.006>

505 Bonnet, J.-L., Bonnemoy, F., Dusser, M., Bohatier, J., 2007. Assessment of the potential
506 toxicity of herbicides and their degradation products to nontarget cells using two
507 microorganisms, the bacteria *Vibrio fischeri* and the ciliate *Tetrahymena pyriformis*.
508 *Environ. Toxicol.* 22, 78–91. <https://doi.org/10.1002/tox.20237>

509 Bonnineau, C., Sague, I.G., Urrea, G., Guasch, H., 2012. Light history modulates antioxidant
510 and photosynthetic responses of biofilms to both natural (light) and chemical
511 (herbicides) stressors. *Ecotoxicology* 21, 1208–1224. [https://doi.org/10.1007/s10646-](https://doi.org/10.1007/s10646-012-0876-5)
512 [012-0876-5](https://doi.org/10.1007/s10646-012-0876-5)

513 Bricheux, G., Le Moal, G., Hennequin, C., Coffe, G., Donnadiou, F., Portelli, C., Bohatier, J.,
514 Forestier, C., 2013. Characterization and evolution of natural aquatic biofilm
515 communities exposed in vitro to herbicides. *Ecotoxicol. Environ. Saf.* 88, 126–134.
516 <https://doi.org/10.1016/j.ecoenv.2012.11.003>

517 Callahan, B.J., McMurdie, P.J., Holmes, S.P., 2017. Exact sequence variants should replace
518 operational taxonomic units in marker-gene data analysis. *ISME J.* 11, 2639–2643.
519 <https://doi.org/10.1038/ismej.2017.119>

520 Callahan, B.J., McMurdie, P.J., Rosen, M.J., Han, A.W., Johnson, A.J.A., Holmes, S.P., 2016.
521 DADA2: High-resolution sample inference from Illumina amplicon data. *Nat.*
522 *Methods* 13, 581–583. <https://doi.org/10.1038/nmeth.3869>

523 Caporaso, J.G., Lauber, C.L., Walters, W.A., Berg-Lyons, D., Lozupone, C.A., Turnbaugh,
524 P.J., Fierer, N., Knight, R., 2011. Global patterns of 16S rRNA diversity at a depth of
525 millions of sequences per sample. *Proc. Natl. Acad. Sci.* 108, 4516–4522.
526 <https://doi.org/10.1073/pnas.1000080107>

527 Carles, L., Gardon, H., Joseph, L., Sanchís, J., Farré, M., Artigas, J., 2019. Meta-analysis of
528 glyphosate contamination in surface waters and dissipation by biofilms. *Environ. Int.*
529 124, 284–293. <https://doi.org/10.1016/j.envint.2018.12.064>

530 Davoren, M.J., Schiestl, R.H., 2018. Glyphosate Based Herbicides and Cancer Risk: A Post
531 IARC Decision Review of Potential Mechanisms, Policy, and Avenues of Research.
532 *Carcinogenesis*. <https://doi.org/10.1093/carcin/bgy105>

533 Dechartres, J., Pawluski, J.L., Gueguen, M., Jablaoui, A., Maguin, E., Rhimi, M., Charlier,
534 T.D., 2019. Glyphosate and glyphosate-based herbicide exposure during the
535 peripartum period affects maternal brain plasticity, maternal behaviour and
536 microbiome. *J. Neuroendocrinol.* e12731. <https://doi.org/10.1111/jne.12731>

537 Drzyzga, D., Lipok, J., 2018. Glyphosate dose modulates the uptake of inorganic phosphate
538 by freshwater cyanobacteria. *J. Appl. Phycol.* 30, 299–309.
539 <https://doi.org/10.1007/s10811-017-1231-2>

540 Duke, S.O., 2015. Perspectives on transgenic, herbicide-resistant crops in the United States
541 almost 20 years after introduction: Perspectives on transgenic, herbicide-resistant
542 crops. *Pest Manag. Sci.* 71, 652–657. <https://doi.org/10.1002/ps.3863>

543 Edgar, R.C., 2016. UNOISE2: improved error-correction for Illumina 16S and ITS amplicon
544 sequencing (preprint). *Bioinformatics*. <https://doi.org/10.1101/081257>

545 E-Phy, 2018. Le catalogue des produits phytopharmaceutiques et de leurs usages, des matières
546 fertilisantes et des supports de culture autorisés en France.
547 <https://ephy.anses.fr/substance/glyphosate> [WWW Document]. URL
548 <https://ephy.anses.fr/substance/glyphosate> (accessed 7.25.18).

549 Eren, A.M., Maignien, L., Sul, W.J., Murphy, L.G., Grim, S.L., Morrison, H.G., Sogin, M.L.,
550 2013. Oligotyping: differentiating between closely related microbial taxa using 16S

551 rRNA gene data. *Methods Ecol. Evol.* 4, 1111–1119. <https://doi.org/10.1111/2041->
552 210X.12114

553 Eren, A.M., Morrison, H.G., Lescault, P.J., Reveillaud, J., Vineis, J.H., Sogin, M.L., 2015.
554 Minimum entropy decomposition: Unsupervised oligotyping for sensitive partitioning
555 of high-throughput marker gene sequences. *ISME J.* 9, 968–979.
556 <https://doi.org/10.1038/ismej.2014.195>

557 Everett, K.D.E., Dickerson, H.W., 2003. *Ichthyophthirius multifiliis* and *Tetrahymena*
558 *thermophila* Tolerate Glyphosate But Not a Commercial Herbicidal Formulation. *Bull.*
559 *Environ. Contam. Toxicol.* 70, 731–738. <https://doi.org/10.1007/s00128-003-0044-y>

560 Fernandes, G., Aparicio, V.C., Bastos, M.C., De Gerónimo, E., Labanowski, J., Prestes, O.D.,
561 Zanella, R., dos Santos, D.R., 2019. Indiscriminate use of glyphosate impregnates
562 river epilithic biofilms in southern Brazil. *Sci. Total Environ.* 651, 1377–1387.
563 <https://doi.org/10.1016/j.scitotenv.2018.09.292>

564 Forlani, G., Pavan, M., Gramek, M., Kafarski, P., Lipok, J., 2008. Biochemical Bases for a
565 Widespread Tolerance of Cyanobacteria to the Phosphonate Herbicide Glyphosate.
566 *Plant Cell Physiol.* 49, 443–456. <https://doi.org/10.1093/pcp/pcn021>

567 García-Torres, T., Giuffré, L., Romaniuk, R., Ríos, R.P., Pagano, E.A., 2014. Exposure
568 Assessment to Glyphosate of Two Species of Annelids. *Bull. Environ. Contam.*
569 *Toxicol.* 93, 209–214. <https://doi.org/10.1007/s00128-014-1312-8>

570 Gilbert, J.A., Jansson, J.K., Knight, R., 2014. The Earth Microbiome project: successes and
571 aspirations. *BMC Biol.* 12. <https://doi.org/10.1186/s12915-014-0069-1>

572 Gonzalez, D., Juárez, Á.B., Krug, C.P., Santos, M., Vera, M.S., 2019. Freshwater periphyton
573 response to technical-grade and two commercial formulations of glyphosate. *Ecol.*
574 *Austral* 29, 020–027.

575 Hadi, F., Mousavi, A., Noghabi, K.A., Tabar, H.G., Salmanian, A.H., 2013. New bacterial
576 strain of the genus *Ochrobactrum* with glyphosate-degrading activity. *J. Environ. Sci.*
577 *Health Part B-Pestic. Food Contam. Agric. Wastes* 48, 208–213.
578 <https://doi.org/10.1080/03601234.2013.730319>

579 Hove-Jensen, B., Zechel, D.L., Jochimsen, B., 2014. Utilization of Glyphosate as Phosphate
580 Source: Biochemistry and Genetics of Bacterial Carbon-Phosphorus Lyase. *Microbiol.*
581 *Mol. Biol. Rev.* 78, 176–197. <https://doi.org/10.1128/MMBR.00040-13>

582 IPBES, 2018. Summary for policymakers of the regional assessment report on biodiversity
583 and ecosystem services for Europe and Central Asia of the Intergovernmental Science-
584 Policy Platform on Biodiversity and Ecosystem Services. M. Fischer, M. Rounsevell,
585 A. Torre-Marín Rando, A. Mader, A. Church, M. Elbakidze, V. Elias, T. Hahn. P.A.
586 Harrison, J. Hauck, B. Martín-López, I. Ring, C. Sandström, I. Sousa Pinto, P.
587 Visconti, N.E. Zimmermann and M. Christie (eds.), Bonn, Germany.

588 Klátyik, S., Takács, E., Mörtl, M., Földi, A., Trábert, Z., Ács, É., Darvas, B., Székács, A.,
589 2017. Dissipation of the herbicide active ingredient glyphosate in natural water
590 samples in the presence of biofilms. *Int. J. Environ. Anal. Chem.* 97, 901–921.
591 <https://doi.org/10.1080/03067319.2017.1373770>

592 Kumar, S., Stecher, G., Li, M., Knyaz, C., Tamura, K., 2018. MEGA X: Molecular
593 Evolutionary Genetics Analysis across Computing Platforms. *Mol. Biol. Evol.* 35,
594 1547–1549. <https://doi.org/10.1093/molbev/msy096>

595 Liao, K., Bai, Y., Huo, Y., Jian, Z., Hu, W., Zhao, C., Qu, J., 2019. Use of convertible flow
596 cells to simulate the impacts of anthropogenic activities on river biofilm bacterial
597 communities. *Sci. Total Environ.* 653, 148–156.
598 <https://doi.org/10.1016/j.scitotenv.2018.10.363>

599 Lima, I.S., Baumeier, N.C., Rosa, R.T., Campelo, P.M.S., Rosa, E.A.R., 2014. Influence of
600 glyphosate in planktonic and biofilm growth of *Pseudomonas aeruginosa*. *Braz. J.*
601 *Microbiol.* 45, 971–975.

602 Lipok, J., Owsiak, T., Mlynarz, P., Forlani, G., Kafarski, P., 2007. Phosphorus NMR as a tool
603 to study mineralization of organophosphonates - The ability of *Spirulina* spp. to
604 degrade glyphosate. *Enzyme Microb. Technol.* 41, 286–291.
605 <https://doi.org/10.1016/j.enzmictec.2007.02.004>

606 Liu, Y.-B., Long, M.-X., Yin, Y.-J., Si, M.-R., Zhang, L., Lu, Z.-Q., Wang, Y., Shen, X.-H.,
607 2013. Physiological roles of mycothiol in detoxification and tolerance to multiple
608 poisonous chemicals in *Corynebacterium glutamicum*. *Arch. Microbiol.* 195, 419–429.
609 <https://doi.org/10.1007/s00203-013-0889-3>

610 Lu, G.-H., Zhu, Y.-L., Kong, L.-R., Cheng, J., Tang, C.-Y., Hua, X.-M., Meng, F.-F., Pang,
611 Y.-J., Yang, R.-W., Qi, J.-L., Yang, Y.-H., 2017. Impact of a Glyphosate-Tolerant
612 Soybean Line on the Rhizobacteria, Revealed by Illumina MiSeq. *J. Microbiol.*
613 *Biotechnol.* 27, 561–572. <https://doi.org/10.4014/jmb.1609.09008>

614 Mcauliffe, K., Hallas, L., Kulpa, C., 1990. Glyphosate Degradation by *Agrobacterium-*
615 *Radiobacter* Isolated from Activated-Sludge. *J. Ind. Microbiol.* 6, 219–221.
616 <https://doi.org/10.1007/BF01577700>

617 Motta, E.V.S., Raymann, K., Moran, N.A., 2018. Glyphosate perturbs the gut microbiota of
618 honey bees. *Proc. Natl. Acad. Sci.* 115, 10305–10310.
619 <https://doi.org/10.1073/pnas.1803880115>

620 NAIADES, 2018. Données sur la qualité des eaux de surface. <http://www.naiades.eaufrance.fr>
621 [WWW Document]. URL [http://www.naiades.eaufrance.fr/acces-](http://www.naiades.eaufrance.fr/acces-donnees#/physicochimie)
622 [donnees#/physicochimie](http://www.naiades.eaufrance.fr/acces-donnees#/physicochimie) (accessed 5.23.18).

623 Peng, Y., Li, J., Lu, J., Xiao, L., Yang, L., 2018. Characteristics of microbial community
624 involved in early biofilms formation under the influence of wastewater treatment plant
625 effluent. *J. Environ. Sci.* 66, 113–124. <https://doi.org/10.1016/j.jes.2017.05.015>

626 Perfilieva, A.I., Pavlova, A.G., Bukhyanova, B.B., Tsvileva, O.M., 2018. Pesticides impact on
627 *Clavibacter michiganensis* ssp. *sepedonicus* biofilm formation. *J. Environ. Sci. Health*
628 *Part B* 53, 464–468. <https://doi.org/10.1080/03601234.2018.1455356>

629 Pipke, R., Schulz, A., Amrhein, N., 1987. Uptake of glyphosate by an *Arthrobacter* sp. *Appl.*
630 *Environ. Microbiol.* 53, 974–978.

631 Rossi, F., Mallet, C., Portelli, C., Donnadieu, F., Bonnemoy, F., Artigas, J., 2019. Stimulation
632 or inhibition: Leaf microbial decomposition in streams subjected to complex chemical
633 contamination. *Sci. Total Environ.* 648, 1371–1383.
634 <https://doi.org/10.1016/j.scitotenv.2018.08.197>

635 Shaw, L.E., Mibbayad, A., Centre for Science, Athabasca University, 1 University Drive,
636 Athabasca, AB, T9S 3A3, Canada, 2016. 2,4-D and Glyphosate affect aquatic biofilm
637 accrual, gross primary production, and community respiration. *AIMS Environ. Sci.* 3,
638 663–672. <https://doi.org/10.3934/environsci.2016.4.663>

639 Staub, J.M., Brand, L., Tran, M., Kong, Y., Rogers, S.G., 2012. Bacterial glyphosate
640 resistance conferred by overexpression of an *E. coli* membrane efflux transporter. *J.*
641 *Ind. Microbiol. Biotechnol.* 39, 641–647. <https://doi.org/10.1007/s10295-011-1057-x>

642 Strayer, D.L., Dudgeon, D., 2010. Freshwater biodiversity conservation: recent progress and
643 future challenges. *J. North Am. Benthol. Soc.* 29, 344–358. [https://doi.org/10.1899/08-](https://doi.org/10.1899/08-171.1)
644 171.1

645 Sviridov, A.V., Shushkova, T.V., Ermakova, I.T., Ivanova, E.V., Epiktetov, D.O.,
646 Leontievsky, A.A., 2015. Microbial degradation of glyphosate herbicides (Review).
647 *Appl. Biochem. Microbiol.* 51, 188–195.

- 648 Sviridov, A.V., Shushkova, T.V., Zelenkova, N.F., Vinokurova, N.G., Morgunov, I.G.,
649 Ermakova, I.T., Leontievsky, A.A., 2012. Distribution of glyphosate and
650 methylphosphonate catabolism systems in soil bacteria *Ochrobactrum anthropi* and
651 *Achromobacter* sp. *Appl. Microbiol. Biotechnol.* 93, 787–796.
652 <https://doi.org/10.1007/s00253-011-3485-y>
- 653 Talbot, H.W., Johnson, L.M., Munnecke, D.M., 1984. Glyphosate utilization by *Pseudomonas*
654 sp. and *Alcaligenes* sp. isolated from environmental sources. *Curr. Microbiol.* 10, 255–
655 259. <https://doi.org/10.1007/BF01577137>
- 656 Tikhonov, M., Leach, R.W., Wingreen, N.S., 2015. Interpreting 16S metagenomic data
657 without clustering to achieve sub-OTU resolution. *ISME J.* 9, 68–80.
658 <https://doi.org/10.1038/ismej.2014.117>
- 659 Tsui, M.T.K., Chu, L.M., 2003. Aquatic toxicity of glyphosate-based formulations:
660 comparison between different organisms and the effects of environmental factors.
661 *Chemosphere* 52, 1189–1197. [https://doi.org/10.1016/S0045-6535\(03\)00306-0](https://doi.org/10.1016/S0045-6535(03)00306-0)
- 662 Tubay, J.M., Ito, H., Uehara, T., Kakishima, S., Morita, S., Togashi, T., Tainaka, K., Niraula,
663 M.P., Casareto, B.E., Suzuki, Y., Yoshimura, J., 2013. The paradox of enrichment in
664 phytoplankton by induced competitive interactions. *Sci. Rep.* 3.
665 <https://doi.org/10.1038/srep02835>
- 666 Van Bruggen, A.H.C., He, M.M., Shin, K., Mai, V., Jeong, K.C., Finckh, M.R., Morris, J.G.,
667 2018. Environmental and health effects of the herbicide glyphosate. *Sci. Total*
668 *Environ.* 616–617, 255–268. <https://doi.org/10.1016/j.scitotenv.2017.10.309>
- 669 Van Horn, D., Sinsabaugh, R., Takacs-Vesbach, C., Mitchell, K., Dahm, C., 2011. Response
670 of heterotrophic stream biofilm -communities to a gradient of resources. *Aquat.*
671 *Microb. Ecol.* 64, 149–161. <https://doi.org/10.3354/ame01515>
- 672 Vera, M.S., Lagomarsino, L., Sylvester, M., Pérez, G.L., Rodríguez, P., Mugni, H., Sinistro,
673 R., Ferraro, M., Bonetto, C., Zagarese, H., 2010. New evidences of
674 Roundup®(glyphosate formulation) impact on the periphyton community and the
675 water quality of freshwater ecosystems. *Ecotoxicology* 19, 710–721.
- 676 Voříšková, J., Baldrian, P., 2013. Fungal community on decomposing leaf litter undergoes
677 rapid successional changes. *ISME J.* 7, 477–486.
678 <https://doi.org/10.1038/ismej.2012.116>
- 679 Zhan, H., Feng, Y., Fan, X., Chen, S., 2018. Recent advances in glyphosate biodegradation.
680 *Appl. Microbiol. Biotechnol.* <https://doi.org/10.1007/s00253-018-9035-0>
- 681

682

Table 1. Prokaryotic and eukaryotic communities richness and diversity. The values of total species richness Chao1 (**A**) and Shannon's diversity index H' (**B**) are reported as the mean \pm SE (n = 3 per condition and sampling date). (**C**) Results of four-way ANOVA carried out with diversity parameters. The four factors were site (Ups vs. Dws), Pwater (LowP vs. HighP), Gwater (LowG vs. HighG) and Time (6, 13 and 27 days), $P < 0.05$. Significant differences (calculated separately for Day 0 and Day 6 to Day 27) are indicated by lowercase letters, $a < b < c < d < e < f$ (Tukey's test, $P < 0.05$).

(A) Total species richness (Chao1)								
	Site	Day 0	Treatment		Day 6	Day 13	Day 27	Day 6 to Day 27 (Mean \pm SE)
			Phosphorus	Glyphosate				
Bacteria	Upstream	948.03 \pm 52.21 (a)	LowP	LowG	719.52 \pm 12.35 (a)	682.67 \pm 47.24 (a)	723.88 \pm 38.54 (a)	708.69 \pm 19.11 (a)
		946.14 \pm 56.95 (a)		HighG	804.07 \pm 52.15 (a)	701.51 \pm 42.17 (a)	792.17 \pm 6.89 (a)	765.91 \pm 25.32 (a)
		940.43 \pm 54.32 (a)	HighP	LowG	737.88 \pm 60.11 (a)	695.69 \pm 19.9 (a)	758.73 \pm 118.37 (a)	730.76 \pm 39.85 (a)
		942.59 \pm 51.51 (a)		HighG	656.35 \pm 50.1 (a)	663.15 \pm 5.58 (a)	695.55 \pm 60.94 (a)	671.69 \pm 23.62 (a)
	Downstream	719.51 \pm 27.7 (b)	LowP	LowG	720.31 \pm 77.59 (a)	660.24 \pm 69.71 (a)	609.66 \pm 71.92 (a)	663.4 \pm 39.92 (a)
		717.24 \pm 26.82 (b)		HighG	811.37 \pm 43.72 (a)	549.02 \pm 18.78 (a)	565.98 \pm 15.62 (a)	642.12 \pm 44.78 (a)
		713.6 \pm 26.63 (b)	HighP	LowG	766.04 \pm 60.3 (a)	655.33 \pm 101.37 (a)	600 \pm 4.13 (a)	673.79 \pm 41.91 (a)
		711.17 \pm 26.49 (b)		HighG	717.07 \pm 56.71 (a)	702.13 \pm 28.36 (a)	608.48 \pm 19.34 (a)	675.89 \pm 25.59 (a)
Eukaryotes	Upstream	154 \pm 9.54 (a)	LowP	LowG	113.67 \pm 9.33 (abc)	92.67 \pm 12.91 (abcde)	145 \pm 3.51 (a)	117.11 \pm 8.94 (a)
		154.5 \pm 9 (a)		HighG	116.83 \pm 3.66 (abc)	85.33 \pm 14.71 (bcdef)	90.67 \pm 8.37 (abcde)	97.61 \pm 6.98 (ab)
		154.33 \pm 9.21 (a)	HighP	LowG	130 \pm 9.02 (ab)	88.33 \pm 11.89 (bcdef)	71 \pm 15.62 (cdef)	96.44 \pm 10.75 (ab)
		154.33 \pm 9.68 (a)		HighG	81.17 \pm 7.25 (bcdef)	102 \pm 2.52 (abcd)	86.67 \pm 6.77 (bcdef)	89.94 \pm 4.29 (ab)
	Downstream	88.67 \pm 3.84 (b)	LowP	LowG	79.33 \pm 17.91 (bcdef)	72.33 \pm 8.09 (cdef)	98 \pm 3.79 (abcd)	83.22 \pm 6.93 (bc)
		89 \pm 4.16 (b)		HighG	76.5 \pm 10.75 (bcdef)	39.67 \pm 3.67 (ef)	35 \pm 4.62 (f)	50.39 \pm 7.46 (c)

89.4 ± 4.55 (b)	HighP	LowG	71.67 ± 10.71 (cdef)	84.33 ± 16.75 (bcdef)	65 ± 7 (cdef)	73.67 ± 6.71 (bc)
90.67 ± 5.78 (b)		HighG	80.44 ± 13.06 (bcdef)	73.44 ± 11.69 (cdef)	50 ± 4.93 (def)	67.96 ± 6.99 (bc)

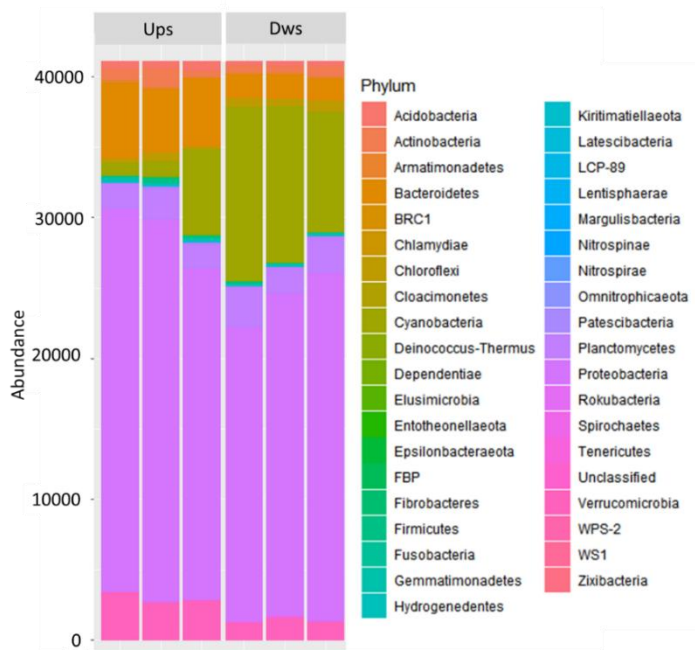
(B) Shannon's diversity index (H')

	Site	Day 0	Treatment		Day 6	Day 13	Day 27	Day 6 to Day 27 (Mean ± SE)
			Phosphorus	Glyphosate				
Bacteria	Upstream	5.89 ± 0.1 (a)	LowP	LowG	5.09 ± 0.22 (a)	5.52 ± 0.14 (a)	5.5 ± 0.01 (a)	5.37 ± 0.1 (a)
		5.89 ± 0.09 (a)		HighG	5.37 ± 0.22 (a)	5.62 ± 0.1 (a)	5.62 ± 0.09 (a)	5.54 ± 0.08 (a)
		5.89 ± 0.1 (a)	HighP	LowG	5.04 ± 0.35 (a)	5.31 ± 0.08 (a)	5.57 ± 0.16 (a)	5.3 ± 0.14 (a)
		5.89 ± 0.1 (a)		HighG	5.04 ± 0.17 (a)	5.32 ± 0.09 (a)	5.34 ± 0.14 (a)	5.24 ± 0.08 (a)
	Downstream	5.15 ± 0.06 (b)	LowP	LowG	5.28 ± 0.12 (a)	5.28 ± 0.09 (a)	5.39 ± 0.11 (a)	5.32 ± 0.06 (a)
		5.15 ± 0.07 (b)		HighG	5.38 ± 0.07 (a)	5.2 ± 0.05 (a)	4.94 ± 0.24 (a)	5.17 ± 0.1 (a)
		5.14 ± 0.07 (b)	HighP	LowG	5.31 ± 0.15 (a)	5.27 ± 0.19 (a)	5.17 ± 0.18 (a)	5.25 ± 0.09 (a)
		5.14 ± 0.07 (b)		HighG	5.2 ± 0.07 (a)	5.38 ± 0.13 (a)	5.03 ± 0.2 (a)	5.2 ± 0.09 (a)
Eukaryotes	Upstream	4.15 ± 0.17 (a)	LowP	LowG	3.63 ± 0.14 (abc)	3.32 ± 0.33 (abcd)	4.11 ± 0.11 (a)	3.68 ± 0.16 (a)
		4.15 ± 0.17 (a)		HighG	3.54 ± 0.13 (abc)	3.21 ± 0.36 (abcd)	3.06 ± 0.3 (abcde)	3.27 ± 0.16 (ab)
		4.16 ± 0.16 (a)	HighP	LowG	3.79 ± 0.19 (ab)	3.11 ± 0.04 (abcde)	2.59 ± 0.24 (bcde)	3.16 ± 0.20 (abc)
		4.14 ± 0.17 (a)		HighG	3.31 ± 0.12 (abcd)	3.18 ± 0.05 (abcd)	3.15 ± 0.07 (abcde)	3.21 ± 0.05 (ab)
	Downstream	3.27 ± 0.11 (b)	LowP	LowG	3.17 ± 0.34 (abcd)	2.95 ± 0.3 (abcde)	3.39 ± 0.05 (abcd)	3.17 ± 0.14 (abc)
		3.27 ± 0.11 (b)		HighG	2.65 ± 0.36 (bcde)	1.94 ± 0.14 (de)	1.7 ± 0.32 (e)	2.10 ± 0.20 (d)
		3.25 ± 0.12 (b)	HighP	LowG	2.88 ± 0.31 (abcde)	2.48 ± 0.41 (bcde)	2.67 ± 0.14 (abcde)	2.68 ± 0.17 (bcd)
		3.27 ± 0.11 (b)		HighG	2.69 ± 0.49 (abcde)	2.33 ± 0.36 (cde)	2.32 ± 0.3 (cde)	2.45 ± 0.20 (cd)

(C) Four-way ANOVA (Day 6 to Day 27)

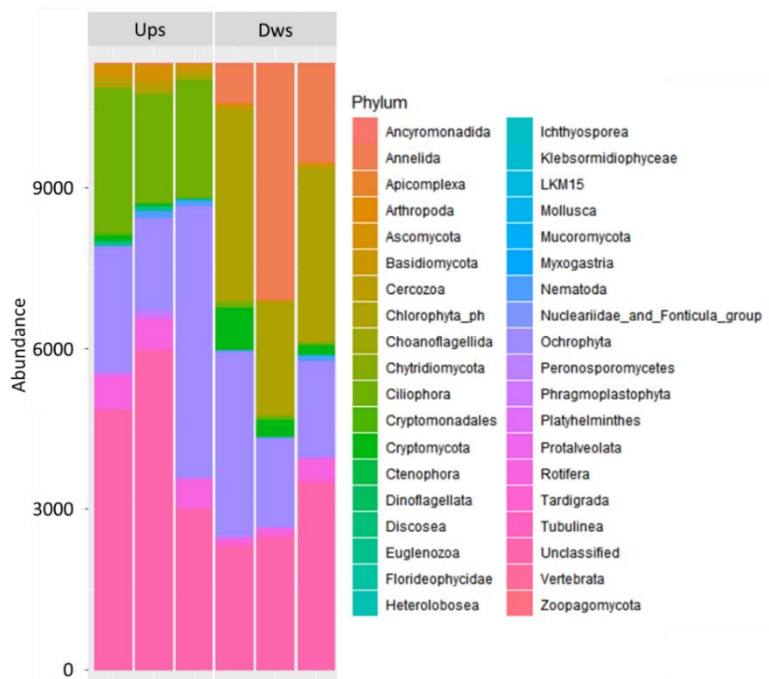
Factor/interaction	Bacteria				Eukaryotes			
	Total species richness (Chao1)		Shannon's H diversity index		Total species richness (Chao1)		Shannon's H diversity index	
	F value	P value	F value	P value	F value	P value	F value	P value
Site	6.366	< 0.05	4.353	< 0.05	57.865	< 0.001	45.846	< 0.001
Pwater	0.101	0.752	2.655	0.11	1.507	0.226	2.75	0.104
Gwater	0.057	0.812	0.137	0.712	15.212	< 0.001	14.725	< 0.001
Time	5.205	< 0.01	1.877	0.164	4.904	< 0.05	5.011	< 0.05
Site*Pwater	1.75	0.192	1.692	0.2	4.826	< 0.05	1.01	0.32
Site*Gwater	0.039	0.845	1.176	0.284	0.574	0.452	4.661	< 0.05
Pwater*Gwater	1.117	0.296	0.353	0.555	5.882	< 0.05	9.022	< 0.01
Site*Time	5.099	< 0.01	5.717	< 0.01	0.722	0.491	0.048	0.953
Pwater*Time	0.975	0.384	0.045	0.956	7.235	< 0.01	0.863	0.429
Gwater*Time	0.166	0.847	1.348	0.27	2.483	0.094	0.965	0.388
Site*Pwater*Gwater	2.524	0.119	1.818	0.184	0.729	0.397	0.748	0.392
Site*Pwater*Time	0.108	0.898	0.56	0.575	0.607	0.549	1.115	0.336
Site*Gwater*Time	0.104	0.901	0.187	0.83	3.791	< 0.05	0.932	0.401
Pwater*Gwater*Time	1.843	0.169	0.511	0.603	7.642	< 0.01	4.055	< 0.05
Site*Pwater*Gwater*Time	0.434	0.656	0.44	0.647	2.394	0.102	0.56	0.575

1 (A)



2

3 (B)



4

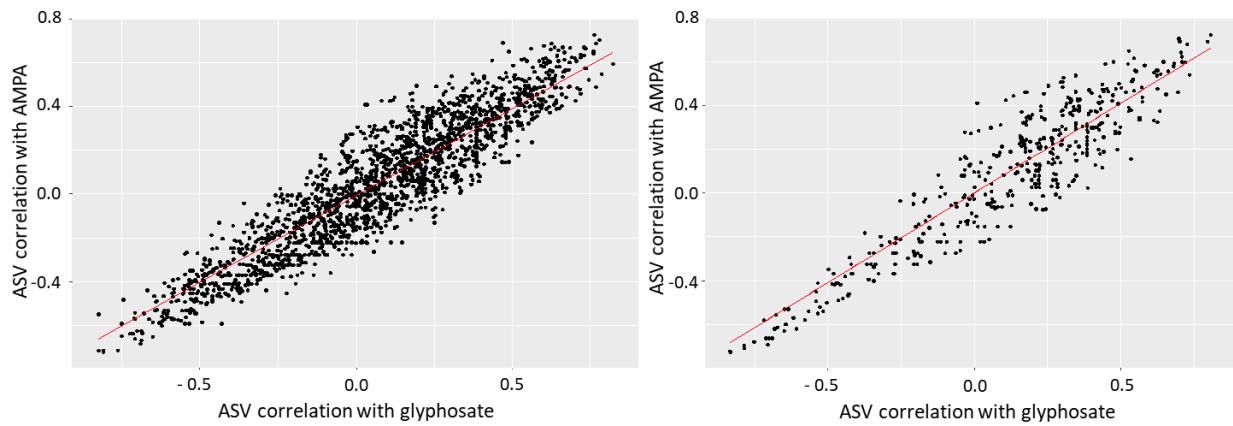
5 **Figure 1.** Microbial community composition of biofilms at the beginning of the experiment at
6 the phylum level. (A) Bacteria; (B) Eukaryotes. Amplicon Sequence Variants (ASVs)
7 abundance for each replicate (n = 3). Ups, Upstream; Dws, Downstream.

8

9
10

(A)

(B)



11
12

13 **Figure 2.** Correlation of Bacterial (A) and Eukaryotic (B) ASVs abundance correlation
14 with glyphosate versus ASVs abundance correlation with AMPA (Spearman). The correlation
15 between ASV abundance and glyphosate (ASV-glyphosate) or AMPA (ASV-AMPA)
16 concentrations has been established over time for bacteria and Eukaryotes using Spearman's
17 rank correlation test. Then, a second correlation test was applied on the correlations ASV-
18 AMPA vs. ASV-Glyphosate (Spearman, red line, bacteria, $\rho = 0.832$, $P < 0.001$; Eukaryotes,
19 $\rho = 0.809$, $P < 0.001$). Each dot represents one ASV.

33 **Supplementary Information**

34

35 **Interaction between glyphosate and dissolved phosphorus on bacterial and eukaryotic**
36 **communities from river biofilms**

37

38

39 Louis Carles^{a*} and Joan Artigas^a

40

41 ^a Université Clermont Auvergne, CNRS, Laboratoire Microorganismes : Génome et
42 Environnement (LMGE), F-63000 Clermont–Ferrand, France

43

44 * Corresponding author:

45 Dr. Louis Carles

46 Now at: Department of Environmental Toxicology (Utox), Swiss Federal Institute of Aquatic

47 Science and Technology (Eawag), Dübendorf, Switzerland.

48 Überlandstrasse 133

49 8600 Dübendorf

50 Switzerland

51 E-mail address: louis.carles@eawag.ch

52 Tel: +41 58 765 54 49

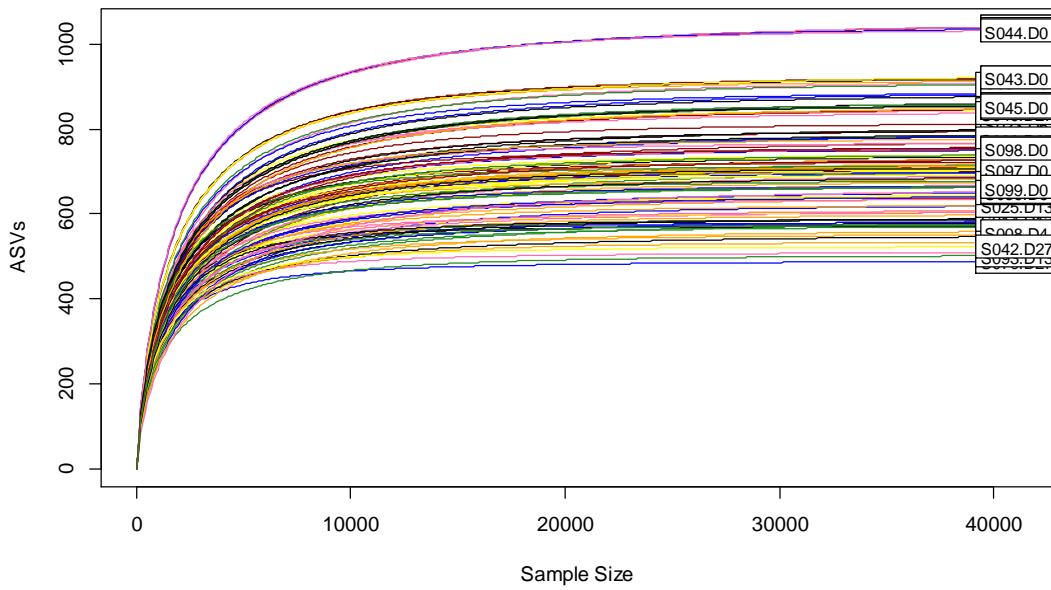
53

54 **Table S1.** Permutational analysis of variance (PERMANOVA) of bacterial and eukaryotic
55 communities richness and diversity. PERMANOVA analyses were carried out on the
56 weighted unfrac distances matrix of bacterial and Eukaryotic communities. The four factors
57 were site (Ups vs. Dws), Pwater (LowP vs. HighP), Gwater (LowG vs. HighG) and Time (6,
58 13 and 27 days), $P < 0.05$.

PERMANOVA				
Factor/interaction	Bacteria		Eukaryotes	
	F value	P value	F value	P value
Site	18.0570	< 0.001	21.8301	< 0.001
Pwater	2.7745	< 0.05	3.8307	< 0.01
Gwater	1.9984	0.054	3.6988	< 0.01
Time	19.8053	< 0.001	5.1685	< 0.001
Site*Pwater	1.4623	0.157	3.0618	< 0.01
Site*Gwater	1.6543	0.125	2.7231	< 0.05
Pwater*Gwater	1.3653	0.191	2.1070	0.059
Site*Time	8.1146	< 0.001	2.4600	< 0.01
Pwater*Time	1.8387	< 0.05	2.7387	< 0.01
Gwater*Time	1.1122	0.306	1.8646	< 0.05
Site*Pwater*Gwater	1.8166	0.077	1.6132	0.147
Site*Pwater*Time	1.1812	0.266	0.8645	0.578
Site*Gwater*Time	0.8411	0.597	1.2296	0.261
Pwater*Gwater*Time	0.8913	0.534	1.6087	0.080
Site*Pwater*Gwater*Time	0.8271	0.619	1.3158	0.206

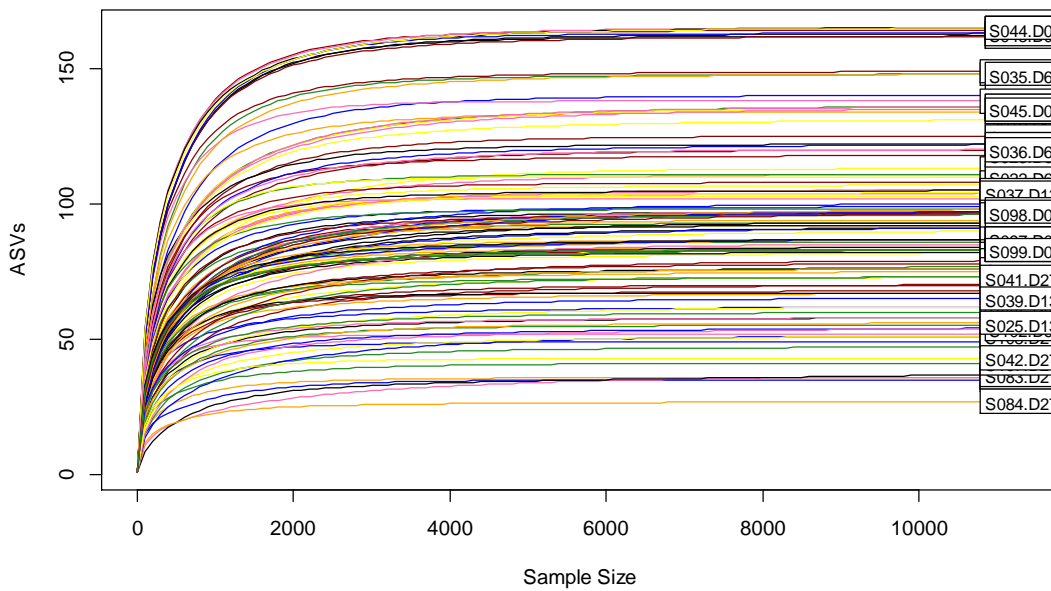
59

60 (A)



61

62 (B)

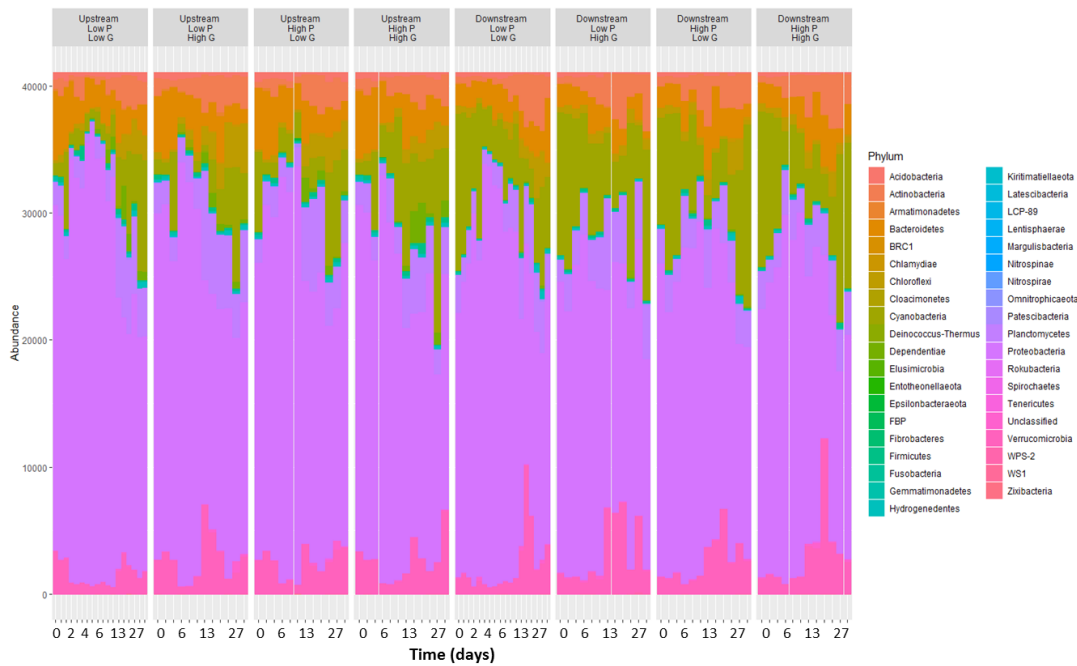


63

64 **Figure S1.** Rarefaction curves of the different set of amplicons. (A) Bacteria; (B)

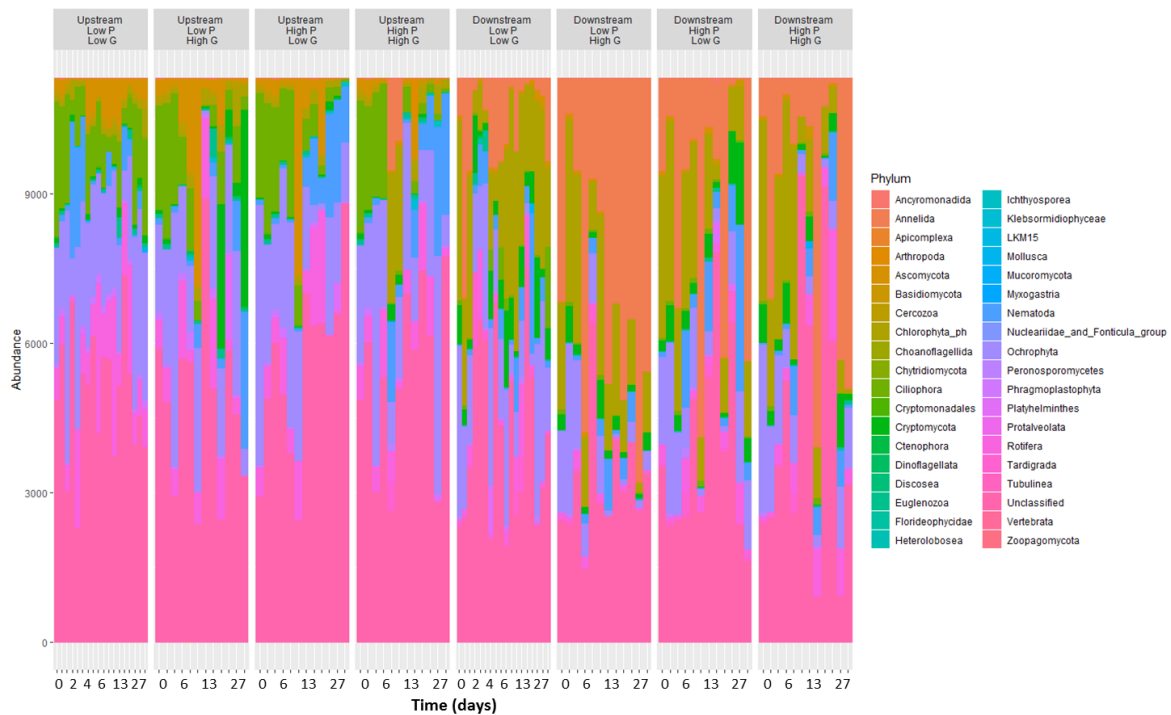
65 Eukaryota. ASVs: Amplicon Sequence Variants.

66 (A)



67

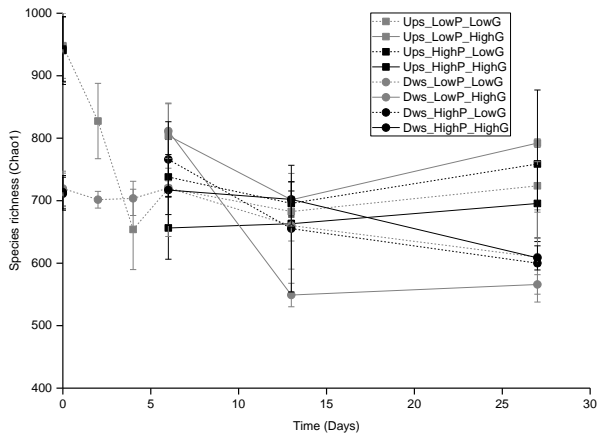
68 (B)



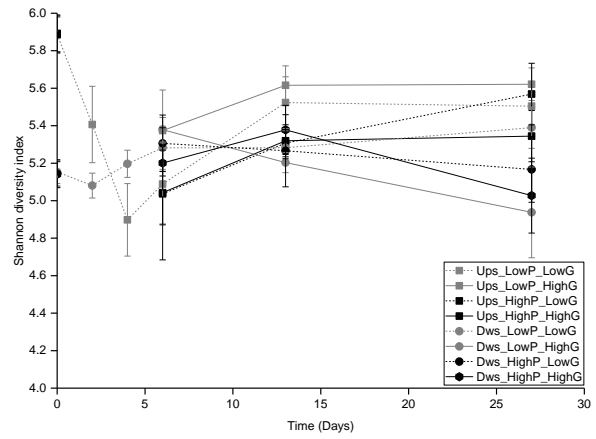
69

70 **Figure S2.** Microbial community composition of biofilms during the experiment at the
 71 phylum level. (A) Bacteria; (B) Eukaryotes. Abundance of Amplicon Sequence Variants
 72 (ASVs) for each replicate (n = 3).

73

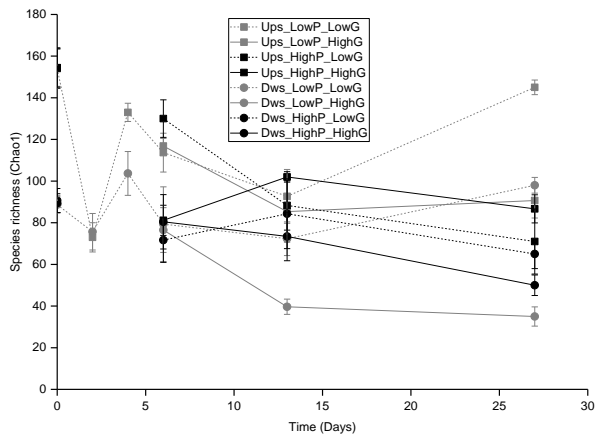


74

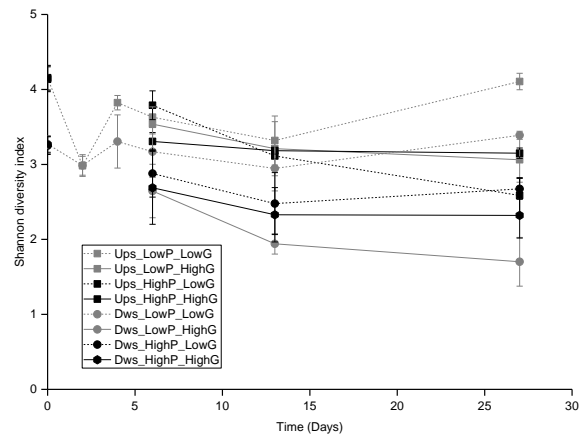


75 (C)

(D)



76



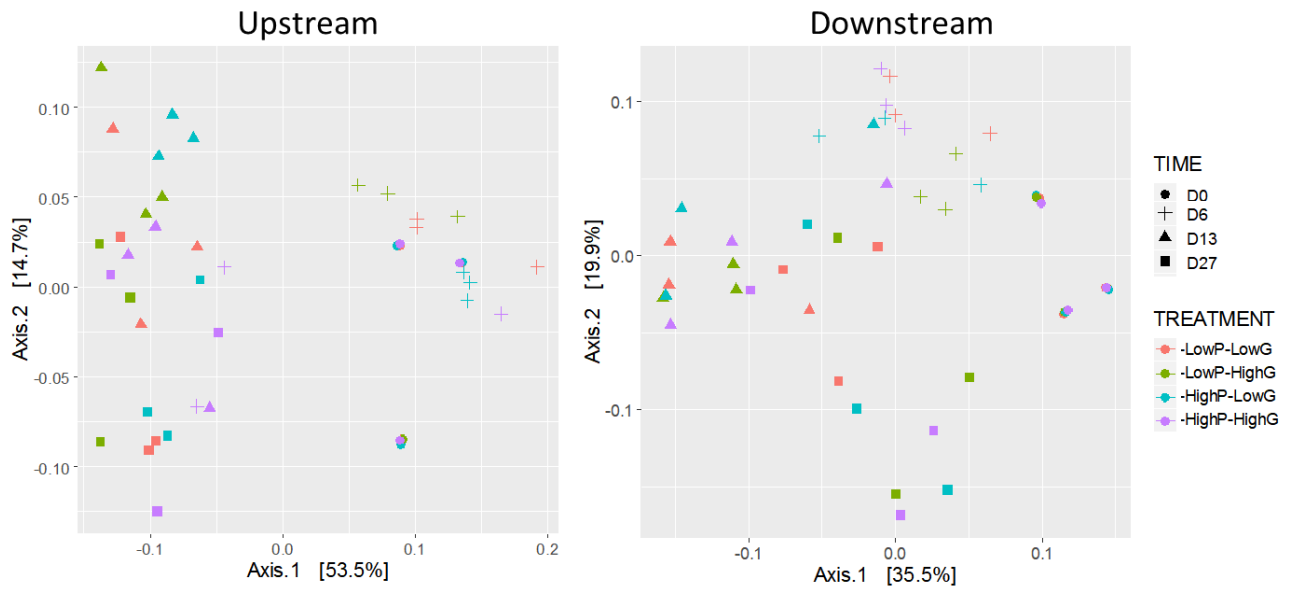
77

78 **Figure S3.** Evolution of microbial communities richness and diversity. Prokaryotes (A)

79 and (B); eukaryotes (C) and (D). The results are reported as the mean \pm standard error (SE), n

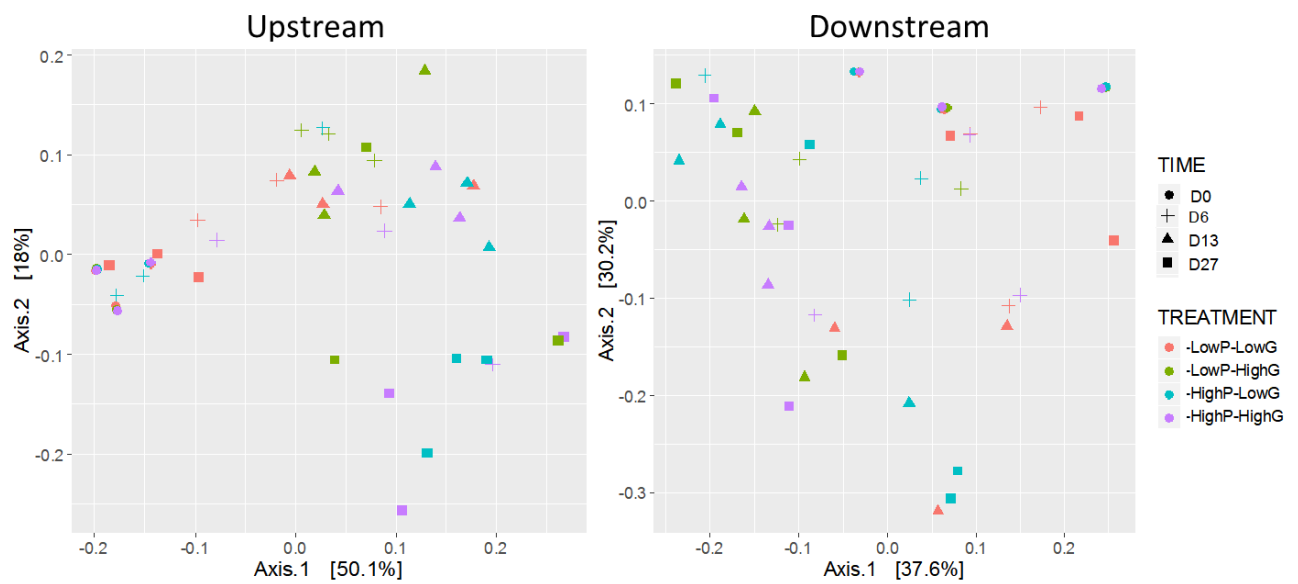
80 = 3.

81 (A)



82

83 (B)



84

85 **Figure S4.** Principal Coordinate Analysis (PCoA) of bacterial (A) and Eukaryotic (B)

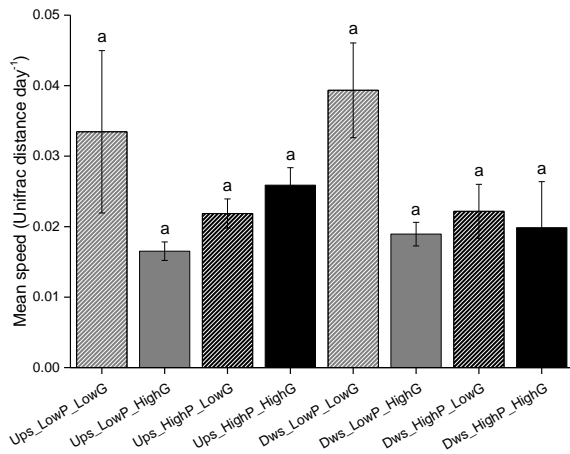
86 communities based on weighted unifracs distances. Results are presented for biofilms grown in

87 upstream and downstream sites of the river. Time in days. Treatments: Phosphorus (LowP vs.

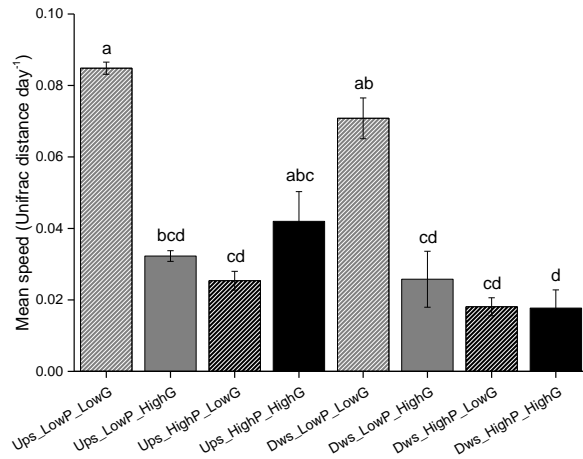
88 HighP) and Glyphosate (LowG vs. HighG).

89

90 (A)



(B)



91

92 **Figure S5.** Mean rate of change in the structure of microbial community during the entire
93 experiment (A, Bacteria; B, Eukaryotes). Speed was calculated as the ratio of Unifrac distance
94 over time. Significant differences are indicated by lowercase letters, $a > b > c > d$ (Tukey's
95 test, $P < 0.05$).

96

97

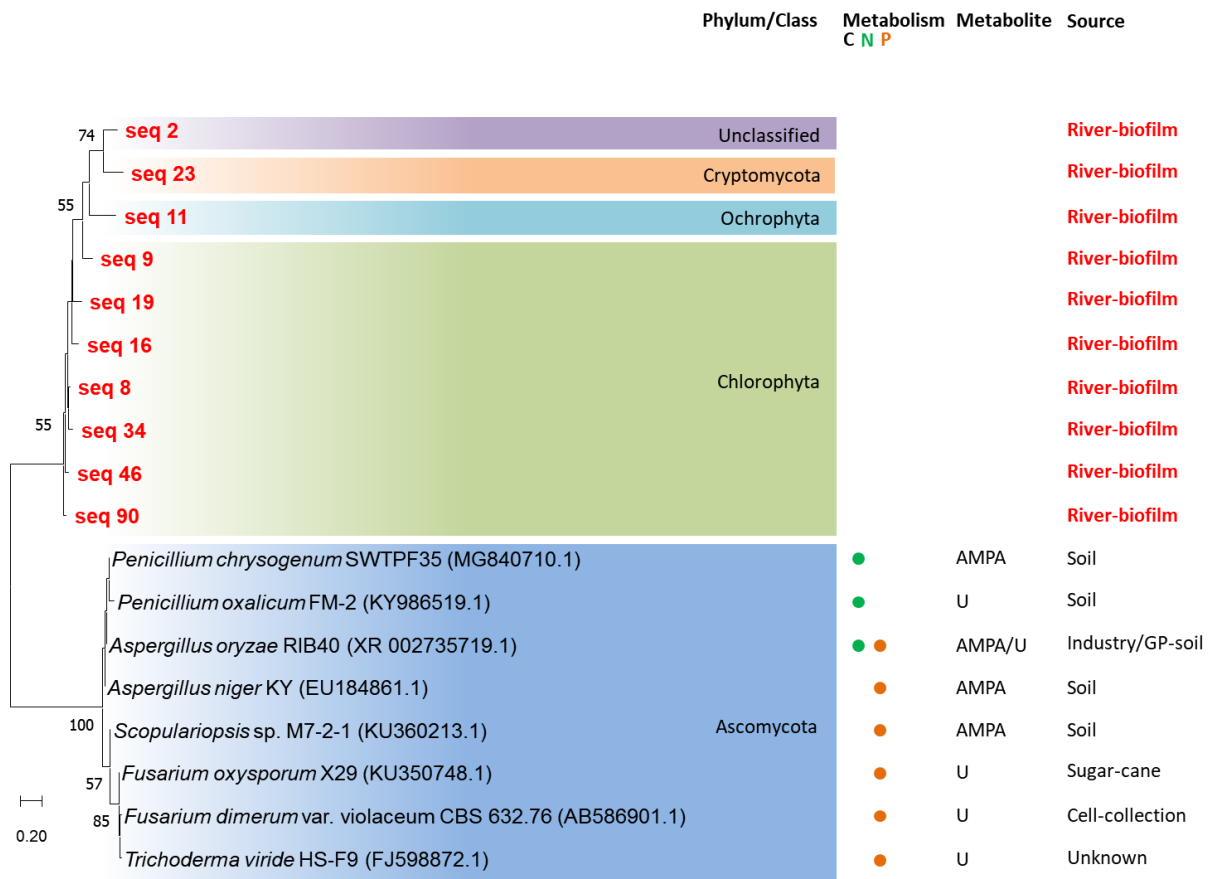


Figure S7. Phylogenetic analysis of the ten highest negatively correlated ASVs with glyphosate (in red, Spearman's rank coefficient < -0.69), together with the known Eukaryotic glyphosate-degrading strains based on 18S gene sequence. The alignment was performed with ClustalW. The tree was constructed with the Neighbor-Joining (N = 1000 bootstrap replicates) using MEGA X. Scale bar = 0.2 substitution per site. Bootstrap percentages $\geq 50\%$ are indicated near tree nodes. For the glyphosate-degrading strains, the metabolism of glyphosate (source of carbon (C), nitrogen (N) and phosphorus (P)) and the main metabolite (AMPA, Sarcosine (S) or unknown (U)) are also indicated on the right.

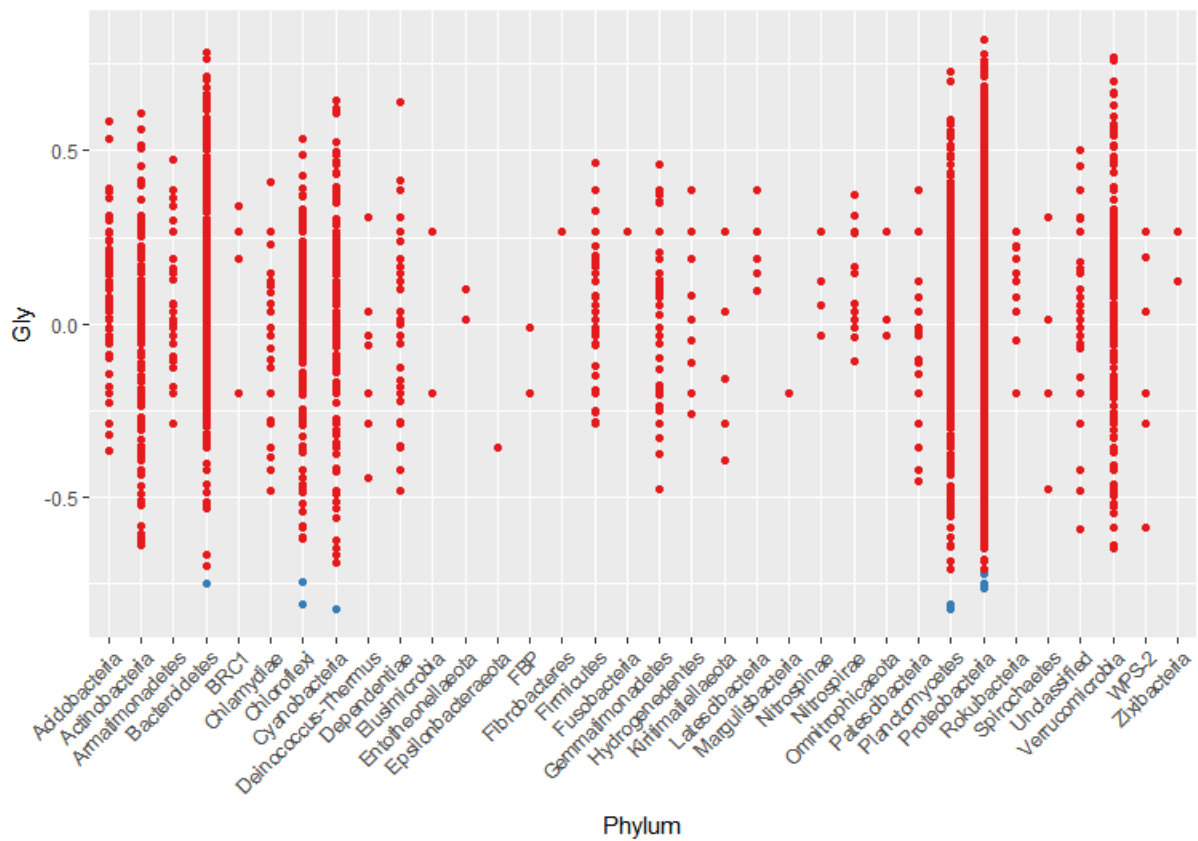


Figure S8. Repartition of the Spearman correlation between bacterial ASVs abundance and glyphosate at the phylum level. Each dot represents the Spearman correlation rank between the abundance of each ASV and the concentration of glyphosate in water. The blue dots correspond to the ASV having negative Spearman's rank coefficient ($r < -0.69$, i.e. present in high abundances when the concentration of glyphosate was drastically decreased in water). These selected ASVs were then proposed as candidates for glyphosate degradation.